# Measurements of $H \rightarrow b\bar{b}$ decays and VH production

Thomas Charman

Supervisor: Dr. Jonathan Hays



Queen Mary University of London

2

I, Thomas Paul Charman, confirm that the research included within this thesis

is my own work or that where it has been carried out in collaboration with, or

supported by others, that this is duly acknowledged below and my contribution

indicated. Previously published material is also acknowledged below.

I attest that I have exercised reasonable care to ensure that the work is original,

and does not to the best of my knowledge break any UK law, infringe any third

party's copyright or other Intellectual Property Right, or contain any confidential

material.

I accept that the College has the right to use plagiarism detection software to

check the electronic version of the thesis. I confirm that this thesis has not been

previously submitted for the award of a degree by this or any other university.

The copyright of this thesis rests with the author and no quotation from it or

information derived from it may be published without the prior written consent of

the author.

Signature:

Date:

Details of collaboration and publications:

## Contents

Li	List of Figures				
Li	st of	Tables	5		
1	Rec	construction and Selection	6		
	1.1	Athena and the CxAOD Framework	6		
	1.2	Leptons	9		
		Electrons	10		
		Muons	10		
		Taus	11		
	1.3	Triggers	11		
		0-lepton channel triggers	12		
		1/2-lepton channel triggers	13		
	1.4	Jets	13		
		Topological Calorimeter Cluster anti- $k_t$ jets	13		
		b-tagging	14		
		Pseudo-continuous b-tagging	16		
		Truth tagging	17		
		Hybrid tagging	19		
	1.5	Missing Transverse Momentum	19		
	1.6	Overlap Removal	22		
	1.7	Final Selection	23		
		0-lepton channel selection	24		

Bibliogra	aphy							27
2	2-lepton channel selection	 	 		 	 	 	25
1	-lepton channel selection	 	 		 	 	 	25

## List of Figures

1.1	A flow chart showing the Athena data processing chain. Red nodes	
	indicate the presence of data recorded from collisions and blue nodes	
	indicate the presence of Monte-Carlo simulated events	7
1.2	A flow chart showing the CxAOD Framework data processing chain. The	
	red elliptical nodes indicate data formats and the blue rectangular nodes	
	indicate software modules	8
1.3	Shapes of the PCBT quantiles for b-,c-, and light-jets	17
1.4	(a) $\Delta R(\text{jet, jet})$ distribution in $t\bar{t}(bb)$ events, (b) $\eta$ distribution in $t\bar{t}(bc)$	
	events and (c) $p_T$ distribution of the leading jet in $t\bar{t}(bl)$ events, using	
	(black) direct tagging, (red) truth tagging and (green) hybrid tagging	
	with the new customized maps.	20

LIST OF TABLES 5

1.5	(a) $m_{bb}$ distribution in $W+bb$ events, (b) $p_T$ of the sub-leading jet for	
	$W+bc$ events and (c) $\Delta R(\text{jet, jet})$ distribution for $W+bl$ events using	
	(black) direct tagging, (red) truth tagging and (green) hybrid tagging	
	with the new customized maps	21

## List of Tables

1.1	Definitions of the VH leptons used to define and select events for the				
	three analysis channels where $d_0^{sig}$ is the measured with respect to the				
	beam line.	9			
1.2	Triggers used during the 2015, 2016, 2017 and 2018 data collection pe-				
	riods, notation like A or D3 denote periods during the year	12			
1.3	Jet selection requirements. Jet cleaning refers to the quality criteria				
	interfaced through the JetCleaningTool CP tool. This tool removes jets				
	in regions where either coherent/sporadic calorimeter noise or beam-				
	induced background fake jets [? ? ]	14			
1.4	$MV2c10\ b-tagging\ Working\ Points\ \dots$	16			
1.5	Summary of the signal event selection in the 0-, 1- and 2-lepton analyses,	26			

## Chapter 1

### Reconstruction and Selection

At the top level events are required to have one Higgs boson candidate and one vector boson candidate. In all cases a Higgs boson candidate is comprised of two b-tagged jets. More on the jet collection and b-tagging strategy used in section 1.4. Vector boson candidates are defined by a number of different decay products defined in section ??, these decay products are triggered on, specific triggers used are discussed in section 1.3. Reconstruction of basic quantities as well as higher level algorithms such as overlap removal are handled by Athena and the CxAOD Framework, more on these in section 1.1. Finally with all quantities reconstructed events are categorised in different analysis regions, these are described in section ??.

#### 1.1 Athena and the CxAOD Framework

Data recorded by the ATLAS detector is passed through the central collaboration software framework Athena before entering the analysis level data processing. Athena is responsible for the steps shown in figure 1.1. As can be seen in the figure Athena processes both data recorded from collisions and Monte-Carlo simulated predictions. Steps up until and including reconstruction are required to transform the raw or simulated read-out of the detector into what are known as physics objects. These physics objects correspond to UV and IR safe descriptions particles and hadron showers e.g. leptons and jets. Given the initial transverse energy of the

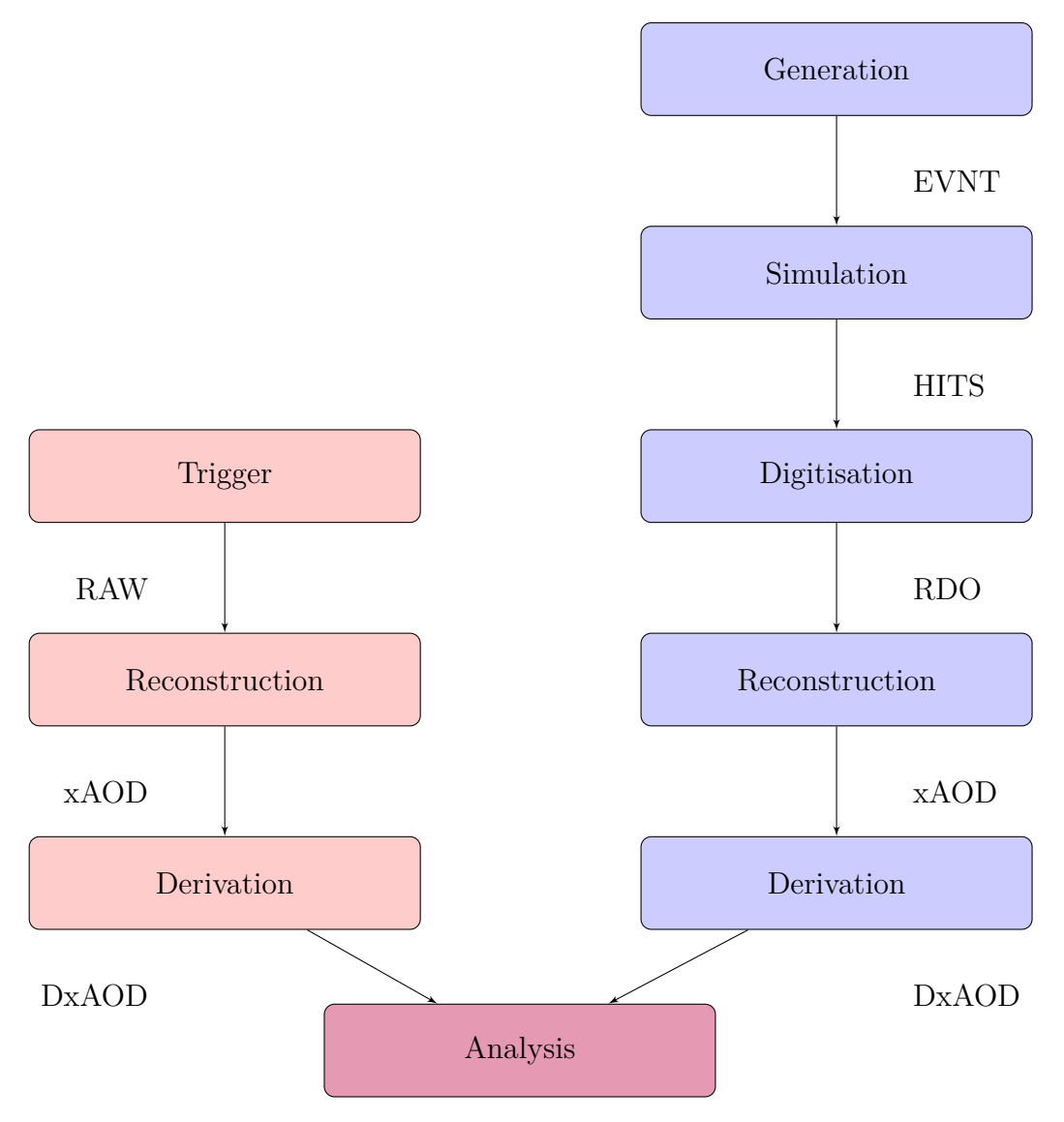


Figure 1.1: A flow chart showing the Athena data processing chain. Red nodes indicate the presence of data recorded from collisions and blue nodes indicate the presence of Monte-Carlo simulated events.

collisions (zero) any missing transverse energy  $(E_{miss}^T)$  is also reconstructed based on the sum of the transverse energy of all objects in an event, this missing energy indicates the presence of particles in the event that cannot be detector by any of ATLAS subsystems. The only particles in the Standard Model for which this is expected are neutrinos. The files containing the reconstructed physics objects adhere to the ATLAS Event Data Model (EDM) and are referred to as Analysis Object Data (xAOD). After reconstruction a part of Athena called the derivation framework is used to produce skimmed and slimmed xAODs known as Derived xAODs (DxAODs). The reduction of these files is carried out based on a loose selection

criteria, the criteria used in the VH(bb) analysis are shown in table ??.

DxAODs are the usual starting point for analysis level software, in the case of this analysis the CxAOD Framework. Of course xAODs can also be used as the starting point for analysis they are just larger. As in in figure 1.2 The CxAOD Framework

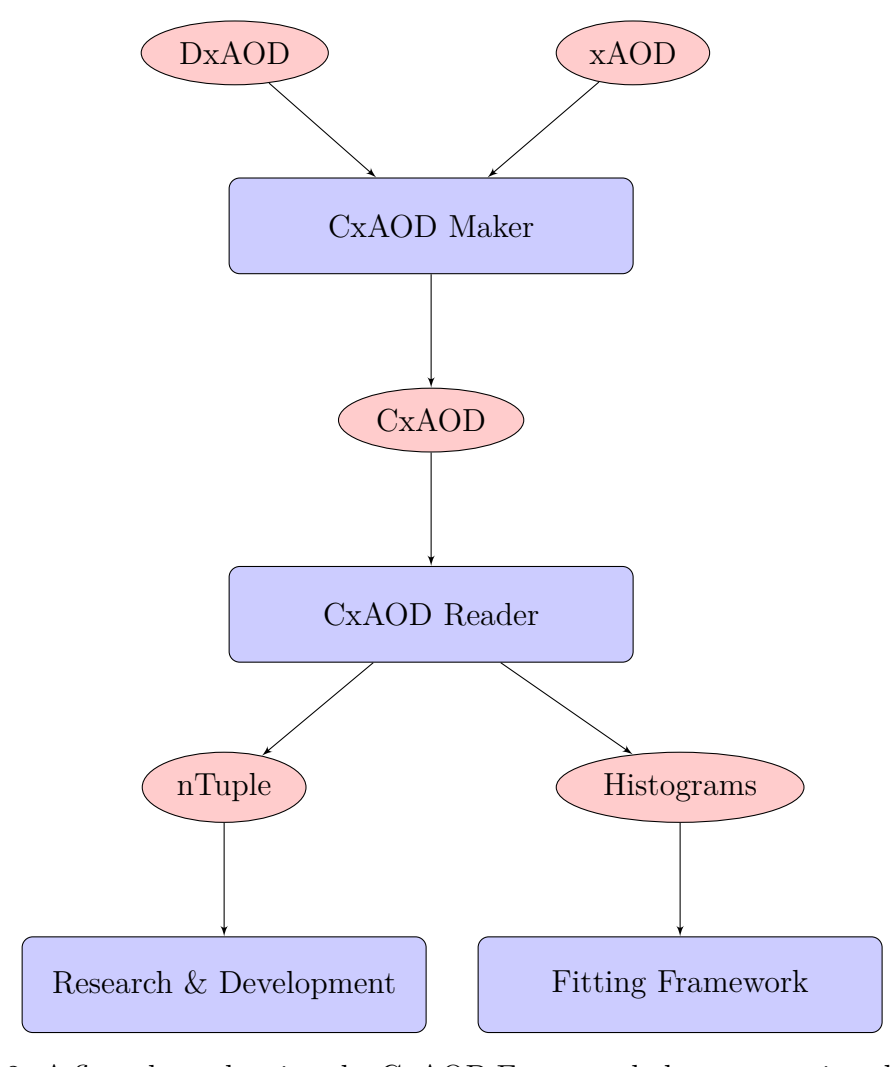


Figure 1.2: A flow chart showing the CxAOD Framework data processing chain. The red elliptical nodes indicate data formats and the blue rectangular nodes indicate software modules.

has two major components the Maker and the Reader. The job of the maker is to further slim the data by performing pre-selection cuts and also to apply calibrations which will be detailed below, the output of the Maker is called a Calibrated xAOD (CxAOD). The Reader takes a CxAOD as input and performs the analysis event selection, it can output histograms or nTuples.

The Maker applies selections the selections of each of the three analysis channels, defined in section ??. CxAODs are produced separately for each of the three

Name	$p_T$	$ \eta $	ID	$d_0^{sig}$	$ \Delta z_0 \sin $	Isolation
electrons						
VH-loose	> 7  GeV	< 2.47	LH Loose	< 5	< 0.5  mm	FCLoose
ZH-signal	> 27  GeV	< 2.47	LH Loose	< 5	< 0.5  mm	FCLoose
WH-signal	> 27  GeV	< 2.47	LH Tight	< 5	< 0.5  mm	${\bf FixedCut HighPtCaloOnly}$
muons						
VH-loose	> 7  GeV	< 2.7	Loose quality	< 3	< 0.5  mm	FixecdCutLoose
ZH-signal	> 27  GeV	< 2.5	Loose quality	< 3	< 0.5  mm	FixecdCutLoose
WH-signal	> 27  GeV	< 2.5	Medium quality	< 3	$<0.5~\mathrm{mm}$	${\bf FixedCutHighPtCaloOnly}$

Table 1.1: Definitions of the VH leptons used to define and select events for the three analysis channels where  $d_0^{sig}$  is the measured with respect to the beam line.

channels as the different background compositions and signal signatures require different optimisation. Pre-selection is performed on jets based on application of requirements on transverse momentum and pseudo-rapidity. A tool known as the Jet Vertex Tagger (JVT) is used to remove jets resulting from pileup from events.

#### 1.2 Leptons

The channels of the VH(bb) analysis are defined by the number of observed charged leptons (e or  $\mu$ ) in the decay of the vector boson. There is one channel for the study of WH(bb) decays where the leptonic decay  $W \to \ell \nu$  yields a single charged lepton. There are two channels for the study of ZH(bb), the zero lepton channel,  $Z \to \nu \nu$ , and the two lepton channel,  $Z \to \ell \ell$ .

Two classifications of lepton are defined in order to categorise events into the individual channels of the analysis, these are called VH-loose and VH-signal leptons, channels are kept orthogonal by requiring different numbers of both lepton categories. These classifications are defined in table 1.1. The characteristics of the fake lepton background from QCD multi-jet processes differs between the 1 and 2 lepton channels hence the reason for two different categorisations. In general to suppress this kind of background leptons are required to be isolated from other detector activity.

#### **Electrons**

As mentioned in chapter ?? electrons leave tracks in the ID and energy deposits in the ECAL. Reconstructing electrons requires clustering the energy deposits in the ECAL, this is achieved with a sliding window algorithm [?]. Clusters must then be associated to tracks in the ID, a Gaussian Sum Filter [?] is used to account for energy loses due to bremsstrahlung radiation. The energy for electron candidates must be calibrated before it can be used in order to account for things such as non-uniformity in the detector response. Calibration is achieved by using simulated cluster activity from single particles to train a BDT regression model designed to regress the measured energy in the ECAL to the simulated energy. An in-situ data driven correction is applied to normalise the response between data and simulation [?].

Reconstruction alone is not enough to find electrons, other particles may leave similar signatures in the ATLAS sub-detectors and therefore electron identification must also be performed. Identification is performed using a likelihood-based method. Variables which have power to discriminate between electrons and other particles are used in the likelihood such as shower profiles, track quality, how closely track and cluster positions match in  $\eta$  and  $\phi$ , and the presence of a high-threshold TRT hit. This is one of the main benefits of the TRT. Performance of this method is well studied [?].

#### Muons

Finding muons in the detector requires consideration of the coverage of the different ATLAS sub-detectors, especially in general are not stopped in the detector. Muons leave charged tracks in the ID and the muon spectrometers which have coverages of  $|\eta| < 2.7$  and  $|\eta| < 2.5$  respectively. For the region  $|\eta| > 2.5$  a stand-alone algorithm which doesn't use ID tracks can be used. All muons within the coverage of the ID require good quality ID tracks []. A combined algorithm is used in the majority of cases. For the region  $|\eta| < 0.1$  two specialised algorithms SegmentTagged and

CaloTagged are used which require only muon segment and calorimeter deposits respectively. All aforementioned algorithms are used together in what is known as a unified chain [?] to reconstruct and identify muons.

#### **Taus**

As mentioned the only charged leptons that are considered in the analysis are electrons and muons, leptonically decaying taus will have electrons and muons as the only visible decay products however hadronically decaying taus must be considered differently. Decays are considered as one or three pronged based on the number of charged decay products, pions, with neutrinos and neutral pions also present. These decays are reconstructed in the calorimeters like jets with the anti- $k_t$  algorithm with  $\Delta R = 0.4$  [?] but the  $p_T$  of the tau is set to the total energy of the TopoClusters within  $\Delta IgoR < 0.2$ , more on TopoClusters in section 1.4. Tau candidates must have  $p_T > 20 GeV$ ,  $|\eta| < 2.5$  excluding  $1.37|\eta| < 1.52$ , and either exactly 1 or 3 tracks. A BDT based method for tau identification is used to reject fakes. Medium quality taus are counted for each event [?].

#### 1.3 Triggers

As stated at the beginning of this chapter the decay products of the vector boson candidate are used to trigger the recording of events for this analysis. Therefore important triggers for the 0-lepton channel are  $E_T^{miss}$  triggers, and for the 1-lepton and 2-lepton channels the single electron, or single muon triggers. Note that it is not necessary to trigger on both charged leptons coming from the Z boson in the 2-lepton channel, the presence of one lepton allows the triggering to occur and the requirement for 2-leptons can be imposed at a later stage. Some events will be missed by not using a di-lepton trigger, however these amount to approximately only 5% of the total. The list of triggers used as they appear in the ATLAS trigger menu are shown in table 1.2, for the  $E_T^{miss}$ , electron and muon triggers respectively.

Trigger Name	Period	Threshold (GeV)	Description
$E_T^{miss}$			
HLT_xe70_L1XE50	2015	70  GeV	Seeded using the level L1_XE50
HLT_xe90_mht_L1XE50	2016 (A-D3)	90  GeV	(L1_XE55) LAr and Tile calorime-
$HLT\_xe110\_mht\_L1XE50$	$2016 \ (\geq D4)$	110  GeV	ter triggers, calibrated at the EM
HLT_xe110_pufit_L1XE55	2017	110  GeV	scale, with a threshold of 50(55)
HLT_xe110_pufit_xe70_L1XE50	2018	110  GeV	GeV.
electrons			
HLT_e24_lhmedium_L1EM20VH	2015	24 GeV	Seeded using L1EM20VH level 1 trigger calibrated at the EM scale with a threshold of 20 GeV, and require medium ID quality.
HLT_e60_lhmedium	2015	$60~{ m GeV}$	Seeded using L1EM20VH level 1 trigger calibrated at the EM scale with a threshold of 20 GeV, and require medium ID quality.
HLT_e120_lhloose	2015	$120~{ m GeV}$	Seeded using L1EM20VH level 1 trigger calibrated at the EM scale with a threshold of 20 GeV, and require loose ID quality.
$HLT\_e26\_lhtight\_nod0\_ivar loose$	2016 - 2018	$26~{\rm GeV}$	Tight likelihood ID required, and variable loose isolation required
HLT e60 lhmedium( nod0)	2016 - 2018	60 GeV	Medium ID likelihood required
HLT e140 lhloose( nod0)	2016 - 2018	140 GeV	Loose ID likelihood required
HLT_e300_etcut	2018	300 GeV	No ID requirements.
muons			
HLT_mu20_iloose_L1MU15	2015	20 GeV	Seeded using L1MU15 level 1 trigger with a threshold of 15 GeV, and requiring loose isolation requirements.
HLT mu50	2015 - 2018	60 GeV	No isolation requirements.
HLT_mu26_ivarmedium	2016 - 2018	26 GeV	Variable cone medium isolation requirements

Table 1.2: Triggers used during the 2015, 2016, 2017 and 2018 data collection periods, notation like A or D3 denote periods during the year.

#### 0-lepton channel triggers

The events in the 0-lepton channel should have a  $qq\nu\nu$  final state. We use the  $E_T^{miss}$  triggers listed in table 1.2 as the final state will manifest in the detector as  $E_T^{miss}$  with the presence of jets. At the stage of triggering  $E_T^{miss}$  is only calculated from energy measured in the calorimeters. As muons do not deposit much energy in the calorimeters the  $W \to \mu\nu$  + jets process is used to study the trigger efficiency and derive an appropriate scale factor.

#### 1/2-lepton channel triggers

The 1 and 2-lepton channels both contain charged leptons in the final state, their final states are specifically  $qq\ell\nu$  and  $qq\ell\ell$  respectively. As the two lepton channel is not expected to contain significant  $E_T^{miss}$  and inefficiencies in the muon trigger are mitigated by the presence of two muons in the events which wish to record the single lepton triggers listed in table 1.2 are simply used without any  $E_T^{miss}$  triggers.

In the 1-lepton channel there is significant  $E_T^{miss}$  expected due to the presence of the neutrino. Single lepton triggers are used for events with  $75GeV < p_T^V < 150GeV$  where the  $E_T^{miss}$  triggers have yet to turn on fully, for events with  $p_T^V > 150GeV$  in order to mitigate inefficiencies in the single muon triggers similar  $E_T^{miss}$  triggers to the 0-lepton triggers are used in conjunction with the single lepton triggers.

#### 1.4 Jets

As mentioned in chapter ?? jets are the roughly conical structure of detector activity resulting from the ultimate hadronisation of a QCD parton. Two categories of jets are considered, signal jets and forward jets, when the number of total jets is referred to it is equal to the sum of signal and forward jets. As the Higgs candidate in every channel of the analysis is two b-tagged jets, both the reconstruction of jets and the b-tagging strategy have huge impacts on the final measurements. In this section the way jets are found and reconstructed will be introduced, b-tagging will be explained in general and then the specific tagging strategy of the analysis will be detailed.

#### Topological Calorimeter Cluster anti- $k_t$ jets

The jets that are found with a given algorithm are referred to as a jet collection. The jet collection relevant to this analysis uses topological calorimeter cell clusters to reconstruct jets [?]. These cluster are then passed to the anti- $k_t$  jet finding algorithm [1]. This algorithm takes a radius parameter which governs the size of jets, in the ATLAS coordinates a radius parameter of R = 0.4 is chosen.

Jet Category	Selection Requirements
Forward Jets	jet cleaning $p_{\rm T} > 30  {\rm GeV}$ $2.5 \le  \eta  < 4.5$
Signal Jets	jet cleaning $p_{\rm T}>20{\rm GeV}$ $ \eta <2.5$ JVT medium for $p_{\rm T}<120{\rm GeV}$

Table 1.3: Jet selection requirements. Jet cleaning refers to the quality criteria interfaced through the JetCleaningTool CP tool. This tool removes jets in regions where either coherent/sporadic calorimeter noise or beam-induced background fake jets [? ?].

As mentioned in chapter ?? pileup can cause issues with reconstruction. In general there is a desire to suppress any jets which arise from pileup. The Jet Vertex Tagger (JVT) is a likelihood-based discriminant which is used to achieve this. The primary vertex location, jet  $p_T$  and the

 $p_T$  of tracks associated to a given jet, serve as inputs to the JVT which outputs a 2-D likelihood that the jet arises from pileup. The likelihood is resilient to bias arising from the jet flavour. The tool is applied only to jets in region  $|\eta| < 2.5$  and  $p_T > 120$  GeV. A cut of JVT = 0.59, is applied to all jets in the collection, this cut has an average efficiency of 92 %. The definitions of signal and forward jets can be found in table 1.3

#### b-tagging

It is important to distinguish jets originating from b-quarks, which form our Higgs candidate, from c-jets and  $\tau$ -jets, as well as jets originating from quarks lighter than c-quark which are categorised together as light-jets. The calculation of a discriminant which ought to separate b-jets from other jets is known as b-tagging. In order to develop such a discriminant one must use simulation in order to be able to know truly which parton initiated a jet such that the performance of the discriminant can be validated. In simulation a jet and the parton that initiated that jet are distinctly separate objects and so a set of rules must be defined in order

to decide which jet is b-jet and likewise for other types of jets. Those rules are as follows:

- 1. If a weakly decaying b-hadron is found within  $\Delta R < R_{\text{max}}$  of the jet axis, the jet is labeled a b-jet.
- 2. If a b-hadron isn't found, but a weakly decaying c-hadron is found within  $\Delta R < R_{\text{max}}$  of the jet axis, then the jet is labeled as a c-jet.
- 3. Otherwise, if a  $\tau$ -lepton is found within  $\Delta R < R_{\text{max}}$  of the jet axis, the jet is labeled a  $\tau$ -jet.
- 4. If any one hadron or  $\tau$ -lepton matches more than one jet, the closest jet is chosen as its parent.
- 5. All unlabeled jets after steps 1 through 4 are labeled as light-jets.

The algorithm used to tag b-jets is the MV2c10 algorithm, this is a BDT which is trained on kinematic and structural information about each jet. It is setup to categorise between b-jets (signal) and a mixture of light-jets and c-jets (background). The events in the training sample are simulated  $t\bar{t}$  events that have at least one lepton coming from a leptonically decaying W boson, and hadronically decaying Z' events. The training sample has 5 million  $t\bar{t}$  events and 3 million Z' events.

The kinematic training variables that enter into the MV2c10 algorithm are simply the jet  $p_T$  and  $\eta$ . The structural information is more complicated, IP2D and IP3D are two algorithms based on a log-likelihood ratio discriminant of impact parameters

(see chapter ??). IP3D is defined as

$$IP3D = \sum_{i=1}^{N} \log \frac{p_b}{p_u} \tag{1.1}$$

where

$$p_b = P\left(\text{is b-jet} \left| \frac{d_0}{\sigma_{d_0}}, \frac{z_0 \sin \theta}{\sigma_{z_0 \sin \theta}} \right),$$
 (1.2)

$$p_u = P\left(\text{is light-jet} \middle| \frac{d_0}{\sigma_{d_0}}, \frac{z_0 \sin \theta}{\sigma_{z_0 \sin \theta}}\right),$$
 (1.3)

and

N = the number of tracks for a given jet.

IP2D has the same definition but the probabilities  $p_b$  and  $p_u$  are conditional only on the transverse impact parameter  $d_0$  and have no dependence on the longitudinal  $z_0$ . The output of two algorithms designed to find secondary vertices, SV1 and JetFitter, also enter into the MV2c10 training.

A jet is defined b-tagged if its MV2c10 score exceeds a certain threshold. This threshold is defined as the cut that gives a pre-determined efficiency value for b-jets when applied to a  $t\bar{t}$  sample. Calibrations are available for a number of these so-called working points, these working points are shown in table 1.4.

Name	MV2c10 cut	b-tagging efficiency (%)	c-jet rejection	light-jet rejection
FixedCutBEff_60	0.94	61.14	22	1204
$FixedCutBEff_70$	0.83	70.84	8	313
$FixedCutBEff\_77$	0.64	77.52	4	113
FixedCutBEff_85	0.11	85.23	2	28

Table 1.4: b-tagging working points available in this analysis, rejection is in the inverse of efficiency.

#### Pseudo-continuous b-tagging

The working points defined in table 1.4 are used in a so-called pseudo-continuous mode. In this mode the MV2c10 distribution is binned with bin edges corresponding to the working points listed in the table, and as can be seen in figure ??. This figure shows the discrimination between events with different jet flavours. Events that

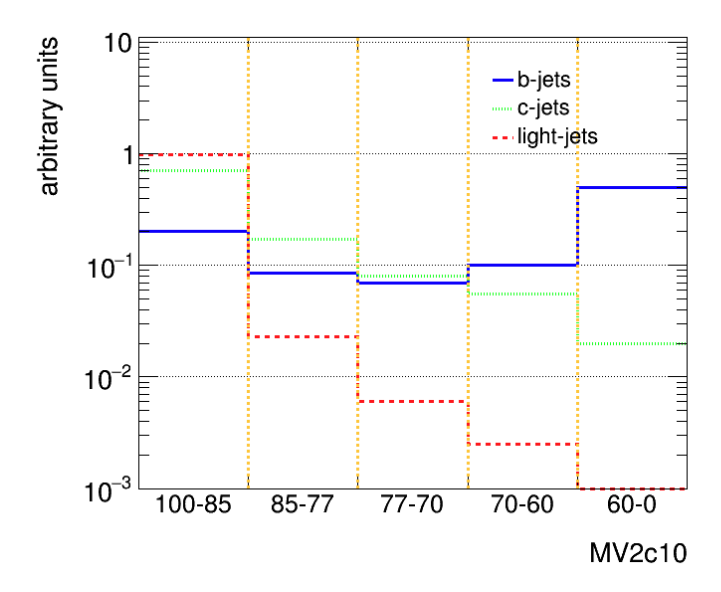


Figure 1.3: Shapes of the PCBT quantiles for b-,c-, and light-jets.

fall in the bins with ranges 70 - 60 % and 60 - 0 % have their MV2c10 score stored for use in the analysis. Events in the other bins are not tagged as b-jets.

#### Truth tagging

Removing all events that fail the cut associated with the 70 % working point results in loss of many events. This leaves us with low statistics samples for analysis where we would rather have high statistics samples, as many of the techniques used for categorising events have performance conditional on the available statistics. Instead of simply throwing these events away it is possible to keep all events that were simulated to have a b-hadron decay and instead weight distributions by a factor which represents the probability that an event would in fact be b-tagged and enter into the final distribution. This procedure is known as Truth-Tagging, since the information as to whether a b-hadron is truly in a simulated event is utilised, this does not use any information relating to the true nature of the data as this is unknowable. In order to draw easy comparisons, tagging directly with the MV2c10 algorithm is referred to as direct tagging.

Given that our events contain more than on jet in all cases it is required to develop of way of generating Truth-Tag weights for events based on all the jets in the event. This weight is calculated as the product of the b-tagging efficiency for each b-tagged jet, multiplied by the complement of the b-tagging efficiency for each non b-tagged jet. In case the number of jets in a given event (m) exceeds the number of required tagged jets in the analysis (n = 2) all possible combinations of jets which satisfy the analysis selection are considered.

Given an event with m jets and n tagged jets required, the possible combinations of tagged and non-tagged jets are  $\binom{m}{n}$ . For a given tagged configuration, referred to as the  $i^{th}$  combination and denoted as  $\binom{m}{n}_i$ , the total number of remaining configurations is  $\overline{\binom{m}{n}} = \binom{m}{n} - \binom{m}{n}_i$ . The efficiency and inefficiency products are

$$\varepsilon\left(\binom{m}{n}_{i}, x, f\right) = \prod_{j \in n} \epsilon_{x}^{f}(j) \tag{1.4}$$

$$\varepsilon_{in}\left(\overline{\binom{m}{n}}_{i}, x, f\right) = \prod_{j \in m-n} (1 - \epsilon_{x}^{f}(j))$$
(1.5)

with  $\epsilon_x^f(j)$  the tagging efficiency of jet j of flavour f at an efficiency working point x, and where  $j \in m-n$  refers to the pool of non tagged jets. The total event weight is

$$w_{TT}(x) = \sum_{i}^{\lfloor \binom{m}{n} \rfloor} \varepsilon \left( \binom{m}{n}_{i}, x \right) \cdot \varepsilon_{in} \left( \overline{\binom{m}{n}}_{i}, x \right), \tag{1.6}$$

with a probability to choose a specific combination equal to

$$P_i(x) = \frac{\varepsilon(\binom{m}{n}_i, x) \cdot \varepsilon_{in}(\overline{\binom{m}{n}_i}, x)}{w_{TT}}.$$
(1.7)

A single truth tagged combination can be selected based on this probability, and the event is then scaled by the factor  $w_{\rm TT}$ . In practice due to differences between the cumulative and pseudo-continuous b-tagging efficiency distributions a modified version of Truth-Tagging must be applied in the analysis, the modifications are described in appendix ??.

#### Hybrid tagging

There exists non-closure between direct-tagged and truth-tagged events which means that truth tagging cannot directly be applied to events in the analysis. This is because direct tagging is the only strategy which can be used on data and so we can only assume that direct-tagged distributions in simulation will describe the shape and normalisation of distributions in the data. This problem is solved by implementing so-called hybrid tagging. The hybrid tagging strategy involves the following steps:

- 1. Divide the jets of each event in two groups, depending on the truth tag flavour: a group with only true b-jets and the other with non b-jets.
- 2. All b-jets in the first group are direct tagged.
- 3. The remaining group of c- and light-jets is truth tagged imposing a number of tagged jets proportional to the difference between the number of required jets in the signal region and the number of true b-jets in the first group passing the b-tag requirement.

Distributions of  $t\bar{t}$  and W + jets are shown in figures 1.4 and 1.5. Which show direct, truth and hybrid-tagged distributions. It can be seen that the closure of hybrid-tagged events is much better than that of truth-tagged events with respect to that of the direct-tagged events. Hybrid tagging is therefore chosen as the analysis strategy.

#### 1.5 Missing Transverse Momentum

This section describes how  $E_T^{miss}$  is calculated. The calculation is based on the assumption that partons entering into the hard scatter interaction have zero transverse momentum when they collide. This is not true due them having Fermi temperature, but the transverse momentum induced by this phenomenon is minimal and therefore is ignored. Given this assumption  $E_T^{miss}$  is calculated as the negative vector sum

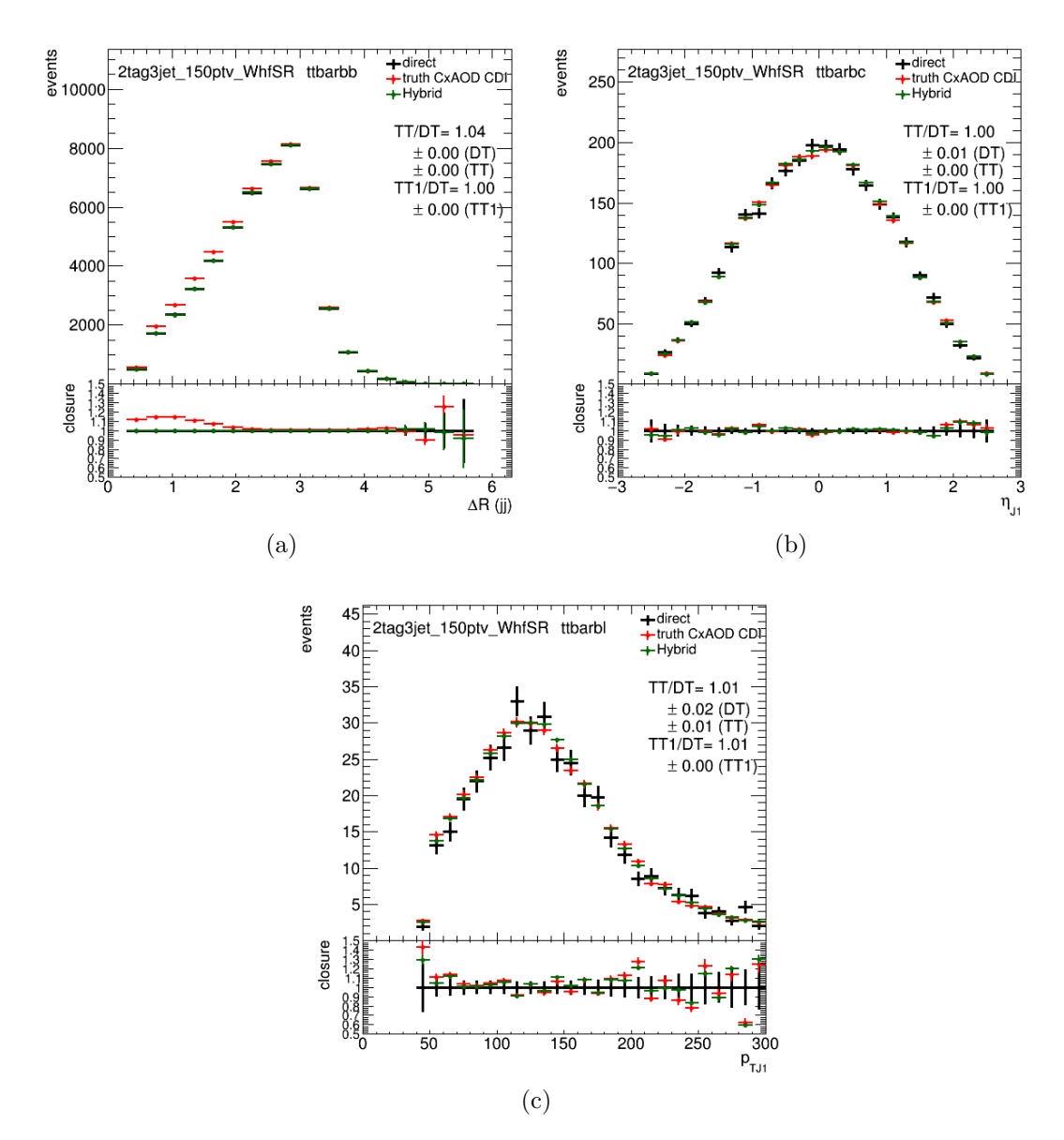


Figure 1.4: (a)  $\Delta R(\text{jet}, \text{jet})$  distribution in  $t\bar{t}(bb)$  events, (b)  $\eta$  distribution in  $t\bar{t}(bc)$  events and (c)  $p_T$  distribution of the leading jet in  $t\bar{t}(bl)$  events, using (black) direct tagging, (red) truth tagging and (green) hybrid tagging with the new customized maps.

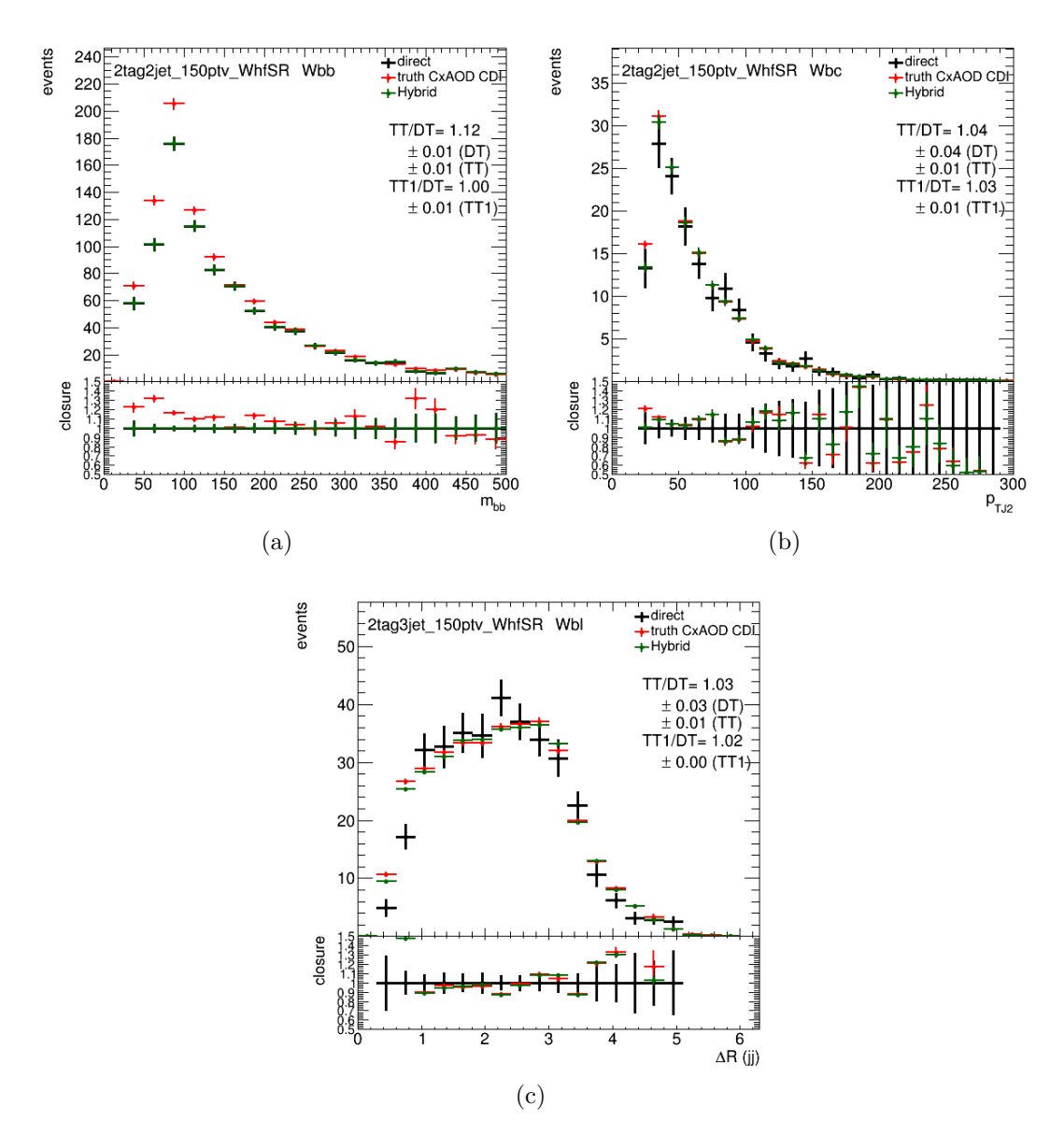


Figure 1.5: (a)  $m_{bb}$  distribution in W+bb events, (b)  $p_T$  of the sub-leading jet for W+bc events and (c)  $\Delta R(\text{jet}, \text{jet})$  distribution for W+bl events using (black) direct tagging, (red) truth tagging and (green) hybrid tagging with the new customized maps.

of the  $p_T$  of photons, electrons, muons, taus, and jets. There is also an additional soft term that enters into the sum which is made up of all good quality tracks that aren't associated with any of the aforementioned objects. These tracks must be associated with the primary vertex and therefore are robust against pileup. A second formulation of  $E_T^{miss}$  called  $E_{T,Trk}^{miss}$  is formulated just using inner detector tracks, it is even more robust to pileup but cannot account for neutral particles which do no leave tracks in the inner detector. One more variable known as  $E_T^{miss}$ -significance is also calculated as

$$E_T^{miss} - \text{significance} = \frac{E_T miss}{\sqrt{\sum p_T^e + \sum p_T^{\mu} + \sum p_T^{jet}}},$$
 (1.8)

where the denominator is clearly proportional to the  $E_T^{miss}$  resolution and therefore making cuts on this variable simulates making harder cuts on  $E_T^{miss}$  with better resolution and looser cuts on  $E_T^{miss}$  with poorer resolution.

#### 1.6 Overlap Removal

Given all of the reconstruction methods described so far for different physics objects there has yet been any mention of what happens if overlapping detector activity could be reconstructed into more than one physics object. The treatment of overlap depends on which physics objects are involved. Below is summary of how different pairs of overlapping objects which are relevant to the analysis are handled, in the summary a combined muon is one which has been reconstructed with the combined muon reconstruction algorithm, that is to say it has tracks in the ID and energy deposits in the ECAL.

- tau-electron: If  $\Delta R(\tau, e) < 0.2$ , the  $\tau$  lepton is removed.
- tau-muon: If  $\Delta R(\tau, \mu) < 0.2$ , the  $\tau$  lepton is removed, unless the  $\tau$  lepton has  $p_T > 50$  GeV and the muon is not a combined muon, then the  $\tau$  lepton is not removed.
- electron-muon: If a combined muon shares an ID track with an electron, the

electron is removed. If a calo-tagged muon shares an ID track with an electron, the muon is removed.

- electron-jet: If  $\Delta R(\text{jet}, e) < 0.2$  the jet is removed. For any remaining jets, if  $\Delta R(\text{jet}, e) < 0.4$ , the electron is removed.
- muon-jet If  $\Delta R(\mathrm{j}et,\mu) < 0.2$  or the muon ID track is ghost associated to the jet, then the jet is removed if the following also holds. The jet has less than three associated tracks with  $p_T > 500$  MeV or the  $p_T$  ratio of the muon and jet is larger than 0.5 and the ratio of the muon  $p_T$  to the sum of  $p_T$  of tracks with  $p_T > 500$  MeV associated to the jet is larger than 0.7. For any remaining jets, if  $\Delta R(\mathrm{jet},\mu) < \min(0.4,0.04+10~\mathrm{GeV}/p_T^{\mu})$ , the muon is removed from the jet.
- tau-jet: If  $\Delta R(\tau, \text{jet}) < 0.2$ , the jet is removed.

#### 1.7 Final Selection

The final analysis selection varies between lepton channels. There are however some common selections to all three channels as the Higgs candidate does not differ between channels, after all this is what we aim to measure. All events must have at least two signal jets. These signal jets must be b-tagged, the b-tagging algorithm used is the MV2c10 algorithm with the 70% efficiency working point used, events with between 0 or 1 b-tags are considered for study and are not used in the final analysis, events with  $\geq 3$  b-tags are rejected entirely. The leading b-tagged jet my have  $p_T > 45$  GeV. A key variable in the analysis, the di-jet mass,  $m_{jj}$  is reconstructed from the two leading jets, in the case where both jets are b-tagged  $m_{bb} \equiv m_{jj}$  and represent the mass of the Higgs candidate.

Reconstruction of the momentum of b-tagged jets can be enhanced with better resolution with respect to other jets. This is achieved with so-called muon-in-jet and  $p_T$ -reco corrections detailed in ??. Corrections are applied after events pass the full analysis selection, but before other stages of the analysis. These corrections are not used in the calculation of any  $E_T^{miss}$  related variables.

#### 0-lepton channel selection

The vector boson candidate in the 0-lepton channel is a Z boson decaying to two neutrinos. In order to select events for this candidate a large amount of  $E_T^{miss}$  is required (> 150 GeV) and there must be exactly 0 VH-loose leptons in the event. Whilst events with lower  $E_T^{miss}$  may come from the physical process we desire to measure the  $E_T^{miss}$  trigger thresholds require setting the cut at it's value, the efficiency is 90% for events with  $E_T^{miss} = 150$  GeV and efficiency plateaus at  $E_T^{miss} \approx 180$  GeV.

There exists a non-trivial dependence of the trigger efficiency on activity of jets in detector. This arises due to the fact that the calculation of  $E_T^{miss}$  is simply the total transverse energy of the event minus the transverse energy of all objects in the event. These effects are hard to model in certain phase spaces and so a requirement is put on  $S_T$  such that it must be greater than 120 GeV for events with two total jets, and greater than 150 GeV for events with three total jets, where  $S_T$  is defined as,

$$S_T = \sum_i p_T^i$$
, for *i* jets in the event. (1.9)

Due to the lack of charged leptons in the  $Z \to \nu\nu$  decay there is nothing to trigger on to suppress multi-jet background processes arising from QCD. This background is also enhanced due to limitations of the calorimeter performance. A set of socalled anti-QCD cuts are applied to deal with this multi-jet background, they are as follows:

- $|\Delta\Phi(E_T^{miss}, E_{t,trk}^{miss})| < 90$
- $|\Delta\Phi(j_1,j_2)| < 140^{\circ}$
- $|\Delta\Phi(E_T^{miss},h)| > 120$ °
- $\min(|\Delta\Phi(E_T^{miss}, \text{pre-sel. jets})|) > 20 \,^{\circ} \text{ for 2 jets}, > 30 \,^{\circ} \text{ for 3 jets}.$

Where  $E_{t,trk}^{miss}$  is defined as the missing transverse momentum calculated from the negative vector sum of the transverse momenta of tracks reconstructed in the inner

detector and identified as originating from the primary vertex. The leading and sub-leading jets are denoted  $j_1$  and  $j_2$ . These cuts reduce the multi-jet background to approximately 1% of the total background in this channel.

#### 1-lepton channel selection

The vector boson candidate in the 1-lepton channel is a W boson decaying to one charged lepton and one neutrino. In order to select for events of this signature exactly one WH-signal lepton is required. At low  $p_T$  there is increased contribution from multi-jet processes, therefore the extra requirements of  $p_T^W > 150$  GeV and  $E_T^{miss} > 30$  GeV. The latter cut is only applied in the electron channel.

#### 2-lepton channel selection

The vector boson candidate in the 1-lepton channel is a W boson decaying to two charged leptons. Exactly two VH-loose leptons of the same lepton flavour are required, additionally one of the leptons must pass the ZH-signal requirements. For events with two muons, it is required that the muons are of opposite charge. Electron reconstruction suffers from a higher rate of charge misidentification and so this requirement is not applied to events with two electrons. The di-lepton invariant mass is confined to be around the Z boson mass peak, events require  $81 < m_{ll} < 101$  GeV. These cuts reduce multi-jet backgrounds to negligible levels.

The presence of two visible leptons in this channel allows for the enhancement to b-tagged jets momentum resolution to be further improved. By inspection of the decay in the channel it is clear that the momentum of the Higgs and vector boson candidates ought to be balanced. The momentum resolution of the two charged leptons forming the Z boson candidate is higher than that of the b-tagged jets forming the Higgs candidate (even after corrections). The b-tagged jets momentum can therefore be corrected with a kinematic fit. The kinematic fit improves resolution by 20-30% compared with the muon-in-jet corrected quantities. This correction is

only applied to events with 2 or 3 total jets as the presence of more jets results in smearing of the effect over those additional jets.

Common Selections	
Jets	$\geq 2$ signal jets
b-jets	2 b-tagged signal jets
Leading b-tagged-jet $p_T$	
Zeading o tagged Jet P1	, 15 661
0 Lepton	
Trigger	lowest un-prescaled $E_T^{miss}$ triggers
Leptons	0 VH-loose lepton
$E_T^{miss}$	> 150 GeV
$S_T^{'}$	> 120 (2 jets), >150 GeV (3 jets)
$ \min \Delta \phi(E_T^{miss}, \text{jet}) $	$> 20^{\circ} (2 \text{ jets}), > 30^{\circ} (3 \text{ jets})$
$ \Delta\phi(E_T^{miss},h) $	> 120°
$ \Delta\phi(j_1,j_2) $	< 140°
$ \Delta\phi(E_T^{miss},E_{T,\mathrm{trk}}^{miss}) $	< 90°
$p_T^V \text{ regions}$	$[150, 250] \text{ GeV}, [250, \infty] \text{ GeV}$
p <sub>T</sub> regions	[150, 250] Gev, [250, 50] Gev
1 Lepton	
Trigger	e channel: un-prescaled single electron
	Tables 6 and 7 of Ref. [?]
	$\mu$ channel: see 0-lepton triggers
Leptons	1 WH-signal lepton
1	> 1 VH-loose lepton veto
$E_T^{miss}$	> 30 GeV (e channel)
$p_T^{V}$ regions	$[150, 250] \text{ GeV}, [250, \infty] \text{ GeV}$
F1 8	[,
2 Lepton	
Trigger	un-prescaled single lepton
	Tables 6 and 7 of Ref. [?]
Leptons	2 VH-loose leptons
-	$(\geq 1 \text{ ZH-signal lepton})$
	Same flavor, opposite-charge for $\mu\mu$
$m_{ll}$	$81 < m_{ll} < 101 \text{ GeV}$
$p_T^{V''}$ regions	$[75,150]$ , $[150, 250]$ , $[250, \infty]$ GeV

Table 1.5: Summary of the signal event selection in the 0-, 1- and 2-lepton analyses.

## Bibliography

[1] Matteo Cacciari, Gavin P. Salam, and Gregory Soyez. The Anti-k(t) jet clustering algorithm. *JHEP*, 04:063, 2008. doi: 10.1088/1126-6708/2008/04/063.